

PSI HELPS TO MAP RELATIVE SUSCEPTIBILITY TO GROUND AND SLOPE INSTABILITIES IN THE LANZHOU LOESS AREA OF GANSU PROVINCE, CHINA

J. Wasowski⁽¹⁾, F. Bovenga⁽²⁾, D.O. Nitti⁽³⁾, R. Nutricato⁽⁴⁾, T. Dijkstra⁽⁵⁾, X. Meng⁽⁶⁾

⁽¹⁾ CNR-IRPI, via Amendola 122 I, 70126 Bari, Italy, Email: j.wasowski@ba.irpi.cnr.it

⁽²⁾ CNR-ISSIA, via Amendola 122 D, 70126 Bari, Italy, Email: bovenga@ba.issia.cnr.it

⁽³⁾ Dipartimento Interateneo di Fisica, Politecnico di Bari, via Amendola 173, 70126 Bari, Italy, Email: davide.nitti@fisica.uniba.it

⁽⁴⁾ GAP srl, c/o Dipartimento Interateneo di Fisica, Politecnico di Bari, via Amendola 173, 70126 Bari, Italy, Email: raffaele.nutricato@gapsrl.eu

⁽⁵⁾ Department of Civil and Building Engineering, Loughborough University, LE11 3TU Loughborough, UK, Email: t.a.dijkstra@lboro.ac.uk

⁽⁶⁾ Research School of Arid Environment and Climate Change, Lanzhou University, Lanzhou, China, Email: xmmeng@lzu.edu.cn

ABSTRACT

The PSI (Persistent Scatterer Interferometry) processing of ENVISAT ASAR data (period 2003-2010) provided spatially dense information (more than 400 PS/km²) on ground surface displacements in Lanzhou, capital of Gansu Province, NW China. The geomorphological and geological context of the local Yellow River valley indicate that the lower, flat areas with floodplain and valley-fill deposits (Holocene terraces with mainly reworked loess at the surface) are stable, whereas some higher, gently sloping valley sides appear locally unstable, particularly where the Late Pleistocene terraces are covered by young aeolian (Malan) loess. The PS velocity data suggest that the relative susceptibility to ground and slope instabilities is the highest on the 4th and 5th order river terraces. This is consistent with the presence of collapsible Malan loess and recent land use of these terraces involving irrigation and construction.

1. INTRODUCTION

Ground and slope instability monitoring and control traditionally rely on qualitative, often subjective geomorphological assessments and, where affordable, on relatively expensive in situ investigations. Due to limited opportunities for *in situ* instrumentation (cost, reliability and robustness) there is often a serious lack of monitoring data. The use of EO (Earth Observation) data, and in particular PSI (Persistent Scatterer Interferometry) results, provides a welcome opportunity to test and calibrate existing ground surface deformation models against independent monitoring data. In turn, a detailed understanding of the behaviour of a surface model, combined with an understanding of the geomorphological and geological context, provides a valuable tool to interpret geotechnical processes.

Here the benefits of PSI applied for ground instability detection and monitoring are for the first time explored for the semi-arid loess area of Lanzhou, capital city of Gansu Province (North-Western China), home to over 3 million people (Fig. 1). In this tectonically active region situated near the eastern fringes of the Tibetan Plateau, landsliding and ground instability in the loess and underlying argillites is widespread and Lanzhou pays an increasingly high price due to lost lives and livelihoods as the city and its environs continue to develop in an unstable terrain [1].

Furthermore, during the last decade, development of the area of interest (and other areas throughout Gansu Province) has resulted in many large-scale engineered interventions, including large infrastructure cut slopes and embankments, and many new construction developments, both domestic and industrial. This offers a unique opportunity to apply PSI to monitor the performance of these interventions and in particular the stability of the recently engineered slopes and built infrastructure.

2. BACKGROUND INFORMATION

2.1. Geomorphology and Geology

The greater Lanzhou area develops for over 300 km² along the Yellow River valley (Fig. 1). The valley is characterized by considerable relative relief (locally exceeding 400 m) and several orders of Late Pleistocene and Holocene river terraces (Figs. 2, 3). Many slopes, including terrace risers, are very steep. In this semi-arid terrain (annual average rainfall highly variable, dependent upon summer monsoon and varying from 150 mm to more than 500 mm per annum, potential evapotranspiration about 1500 mm per annum) vegetation is sparse and requires irrigation support.

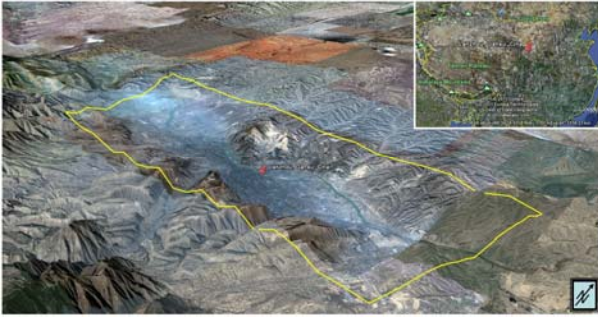


Figure 1. Google Earth view of the greater Lanzhou area that develops along the Yellow River valley. The yellow rectangle (approximately 10 x 30 km) marks the area for which PS information is available. Inset shows location of the city of Lanzhou in north-western China (Gansu Province).

The Lanzhou region is marked by the presence of a drape of aeolian silt deposits (loess) of Quaternary age that cover planated and undulating bedrock surfaces of a range of geologies (Fig. 3), including Miocene/Pliocene argillites and pre-Neogene granites, metamorphic rocks and well lithified sandstones [1]. Locally, loess thickness exceeds 300 m, thicknesses of 50 to 100 m are common. The Lanzhou region is tectonically active and is frequently hit by moderate-large magnitude earthquakes [1]. Bedrock geology is therefore characterised by well developed fault systems and shear zones that extend into the Quaternary loess deposits. Due to a combination of steep slopes, collapsible loess, seismic activity, irregular rainfall and irrigation, landslides represent a common hazard in Lanzhou. For further information on the Lanzhou area geology and environmental setting the interested reader is referred to a comprehensive study by [1] and references therein.

3. INSAR DATASET AND PROCESSING

More than 40 ENVISAT ASAR descending images (period 2003-2010) were processed to obtain stacks of co-registered differential SAR interferograms (Fig. 4). The SPINUA algorithm ([2], [3]) was used to perform multi temporal analysis on the co-registered DInSAR stacks in order to correct for spurious effects such as atmospheric artifacts and DEM errors, and obtain precise displacement information over selected radar persistent targets (PS). The analysis resulted in the identification of over 140,000 PS in the greater Lanzhou area, which amounts to about 300 km² (Fig. 5).

The SPINUA algorithm is a PSI-like technique developed through a joint effort of the Remote Sensing Group of the Department of Physics at Politecnico di Bari and the ISSIA-CNR institute. The algorithm was originally developed with the aim of detection and monitoring of coherent PS targets in scarcely-urbanized

areas. It adopts a patch-wise processing scheme consisting in processing small image patches (usually a few km²) selected according to the density and the distribution of potential PS. This solution enables to obtain fast results on small areas by processing even scarcely populated stacks of SAR images. The SPINUA algorithm has been successfully used to study different geophysical phenomena (landslides, subsidence, post-seismic deformations) and recently has been updated in order to properly process high-resolution X-band data from both COSMO/SkyMed and TSX sensors.

4. INTERPRETATION OF PSI RESULTS

The analysis of the PSI results relied on the integration of radar data with existing optical imagery (from Google Earth), thematic information (e.g. geological, geomorphological, land use maps) and reconnaissance field checks. This helped to assess the likely significance of ground deformations detected in areas potentially susceptible to landsliding, settlements or subsidence, and structural instability.

4.1. Wide-area evaluation

Fig. 5 reveals that, overall, Lanzhou is characterized by a high density of PS (more than 400/km²). This is not surprising considering the urban nature of the area studied and the semi-arid setting with scarce vegetation. Fig. 5 also shows that the great majority of radar targets at Lanzhou exhibit the average Line of Sight (LOS) velocities within ± 2 mm/yr; we assume that these PS are motionless and indicative of stability conditions. It follows that the central (and major) part of the city is unaffected by instabilities. Nevertheless, the PSI displacement map reveals several zones, characterized by the presence of slowly moving PS (with average velocities typically below 10 mm/yr).

When put in a geological and geomorphological context it appears that the PSI results of the Yellow River valley in Lanzhou indicate stable surfaces on the lower, flat areas with floodplain and valley-fill deposits (Holocene terraces of the Yellow River with mainly reworked loess at the surface). Conversely, some higher, gently sloping areas appear locally unstable, particularly where the Late Pleistocene terraces are covered by young aeolian Malan loess (cf. Figs. 2, 3 and 5).

A relatively small number of moving PS were identified on the steep slopes in collapsible, aeolian loess. These slopes are known to be susceptible to instability. However, failure is often catastrophic and capturing pre-failure deformations in these 'brittle' materials is therefore difficult. Also, these particular slopes of interest show a lower density of PS information, because they are characterized by lower degree of urbanization.

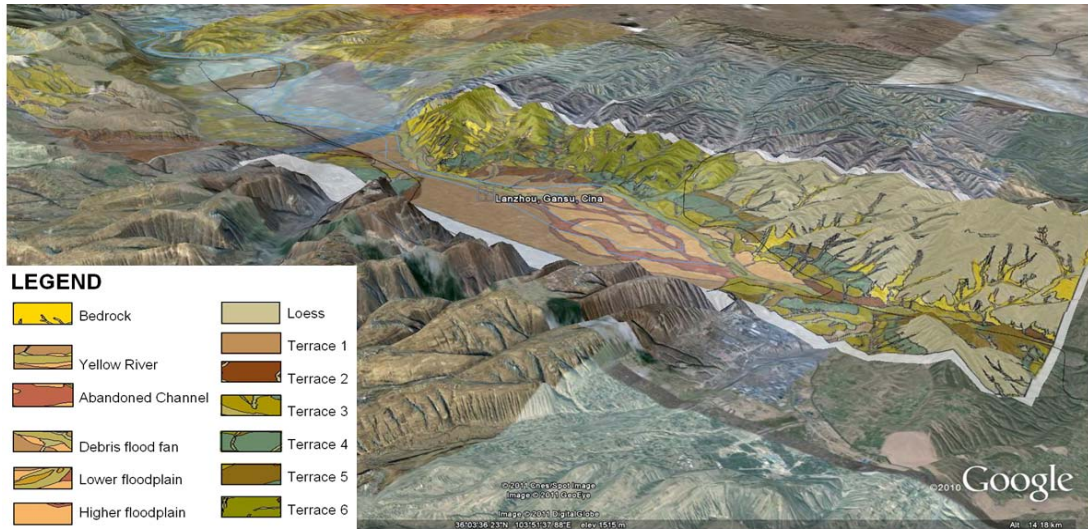


Figure 2. Geomorphological context of the Lanzhou area (after [1]) visualized using Google Earth tools.

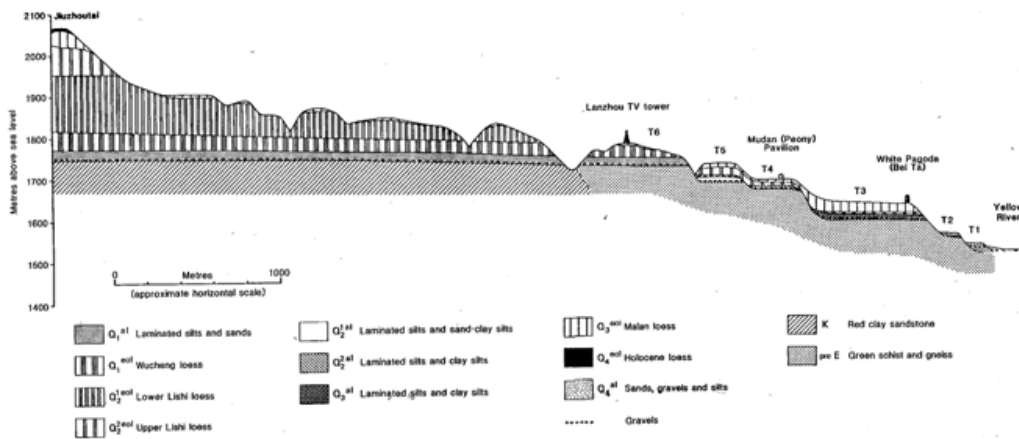
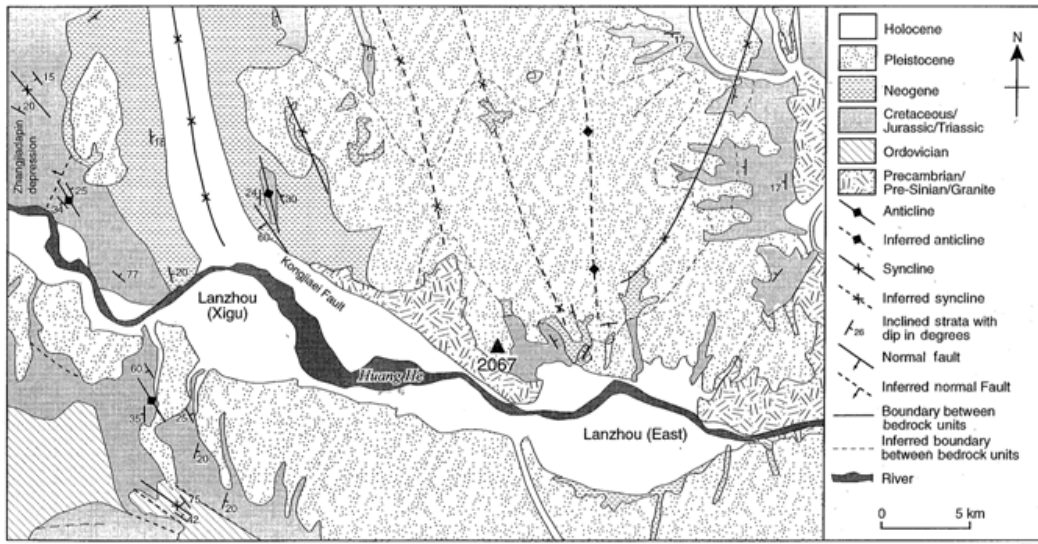


Figure 3. (upper) Geology of the Lanzhou area (from [1]). Huang He = Yellow River. (lower) Simplified geological section illustrating loess sequences in the Lanzhou area (from [1]). Note series of river terraces (T1 being youngest and T6 oldest).

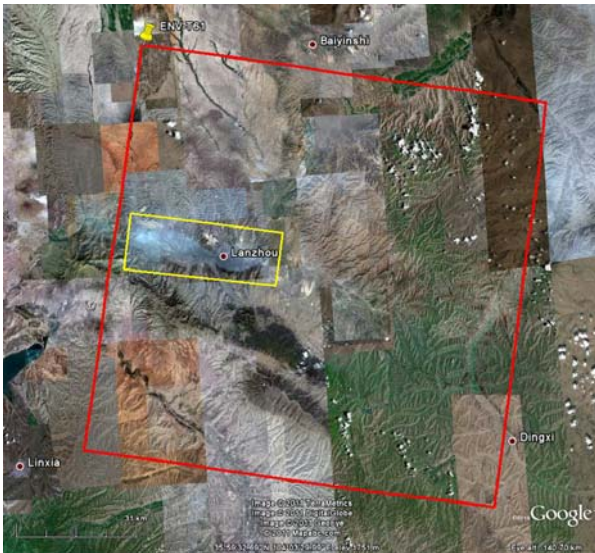


Figure 4. Ground coverage by ENVISAT ASAR images acquired between 16/08/2003 and 27/03/2010 along ascending passes (Track = 61) indicated by red rectangle; study area is outlined in yellow. Background optical image is from Google Earth.

Furthermore, PS with higher velocities appear to occur predominantly on the 4th and 5th order terraces and secondarily on the 3rd terraces. At places the presence of higher velocity PS clusters along the steep terraces risers denotes their instability. This is illustrated in Fig. 6, where the PS velocity information is overlain on the geomorphological map of the eastern Lanzhou.

5. INTERPRETATION OF PSI RESULTS

The analysis of the PSI results relied on the integration of radar data with existing optical imagery (from Google Earth), thematic information (e.g. geological, geomorphological, land use maps) and reconnaissance field checks. This helped to assess the likely significance of ground deformations detected in areas potentially susceptible to landsliding, settlements or subsidence, and structural instability.

5.1. Wide-area evaluation

Fig. 5 reveals that, overall, Lanzhou is characterized by a high density of PS (more than 400/km²). This is not surprising considering the urban nature of the area studied and the semi-arid setting with scarce vegetation. Fig. 5 also shows that the great majority of radar targets at Lanzhou exhibit the average Line of Sight (LOS) velocities within ± 2 mm/yr; we assume that these PS are motionless and indicative of stability conditions. It follows that the central (and major) part of the city is unaffected by instabilities. Nevertheless, the PSI displacement map reveals several zones, characterized

by the presence of slowly moving PS (with average velocities typically below 10 mm/yr).

When put in a geological and geomorphological context it appears that the PSI results of the Yellow River valley in Lanzhou indicate stable surfaces on the lower, flat areas with floodplain and valley-fill deposits (Holocene terraces of the Yellow River with mainly reworked loess at the surface). Conversely, some higher, gently sloping areas appear locally unstable, particularly where the Late Pleistocene terraces are covered by young aeolian Malan loess (cf. Figs. 2, 3 and 5).

A relatively small number of moving PS were identified on the steep slopes in collapsible, aeolian loess. These slopes are known to be susceptible to instability. However, failure is often catastrophic and capturing pre-failure deformations in these 'brittle' materials is therefore difficult. Also, these particular slopes of interest show a lower density of PS information, because they are characterized by lower degree of urbanization.

Furthermore, PS with higher velocities appear to occur predominantly on the 4th and 5th order terraces and secondarily on the 3rd terraces. At places the presence of higher velocity PS clusters along the steep terraces risers denotes their instability. This is illustrated in Fig. 6, where the PS velocity information is overlain on the geomorphological map of the eastern Lanzhou.

5.2. Example of local scale evaluation

Reconnaissance field checks proved that the PSI results provided useful, local scale information on the presence of ground and structure instabilities. For instance this was the case of the movements detected in a small satellite settlement (Dongpingcun) situated in the southern periphery of the western district (Xigu) of Lanzhou (Fig. 7). The settlement is built on terrace T4 which is covered by collapsible Malan loess and our field checks indicated that PS motion (on the order of few to several mm/year) most likely reflects localized subsidence and structural instability. It is also apparent that the deformations tend to concentrate along a drainage corridor running through the central part of the town. It is observed that, in this case, infiltration of excess water and leaking pipework are most likely to contribute to the hydroconsolidation of Malan loess and the subsequent settlement of surface structures. More detailed *in situ* inspections would be needed to better assess the exact cause(s) of the detected movements. Nevertheless, the PS information alone is of much value as it provides a local scale indication of relative susceptibility to ground/structure instability.

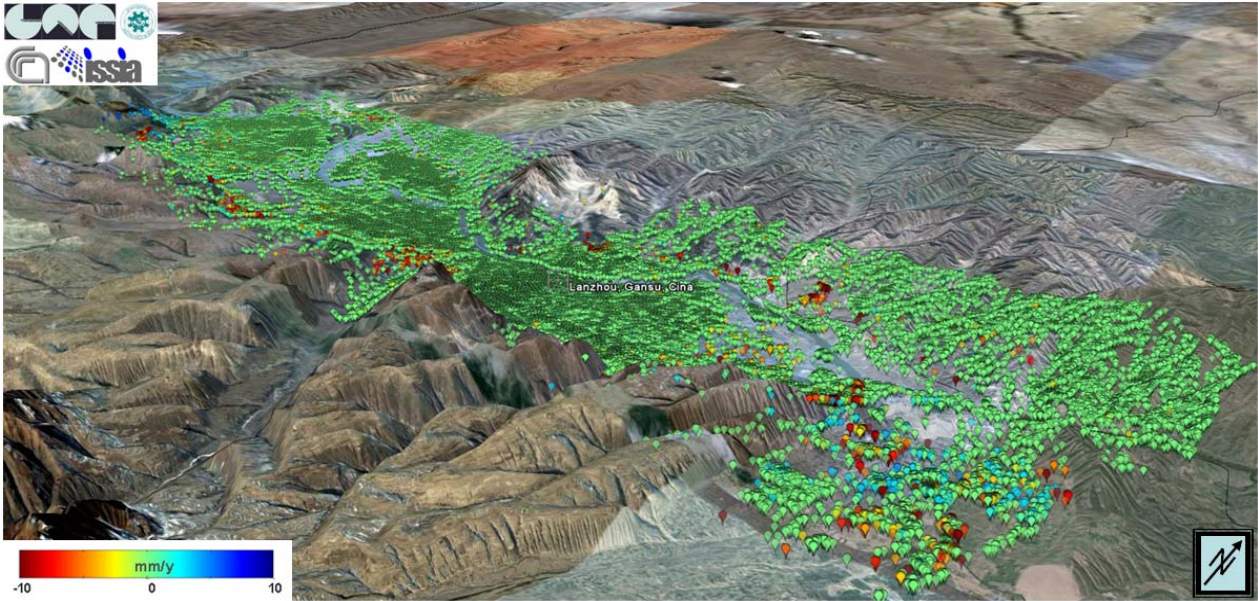


Figure 5. PS mean velocity map of the greater Lanzhou area obtained by processing ENVISAT ASAR data; the Line of Sight (LOS) velocity is saturated between -10 mm/y (red) and 10 mm/y (dark blue). Over 140,000 PS were identified in an area of approximately 300 km².

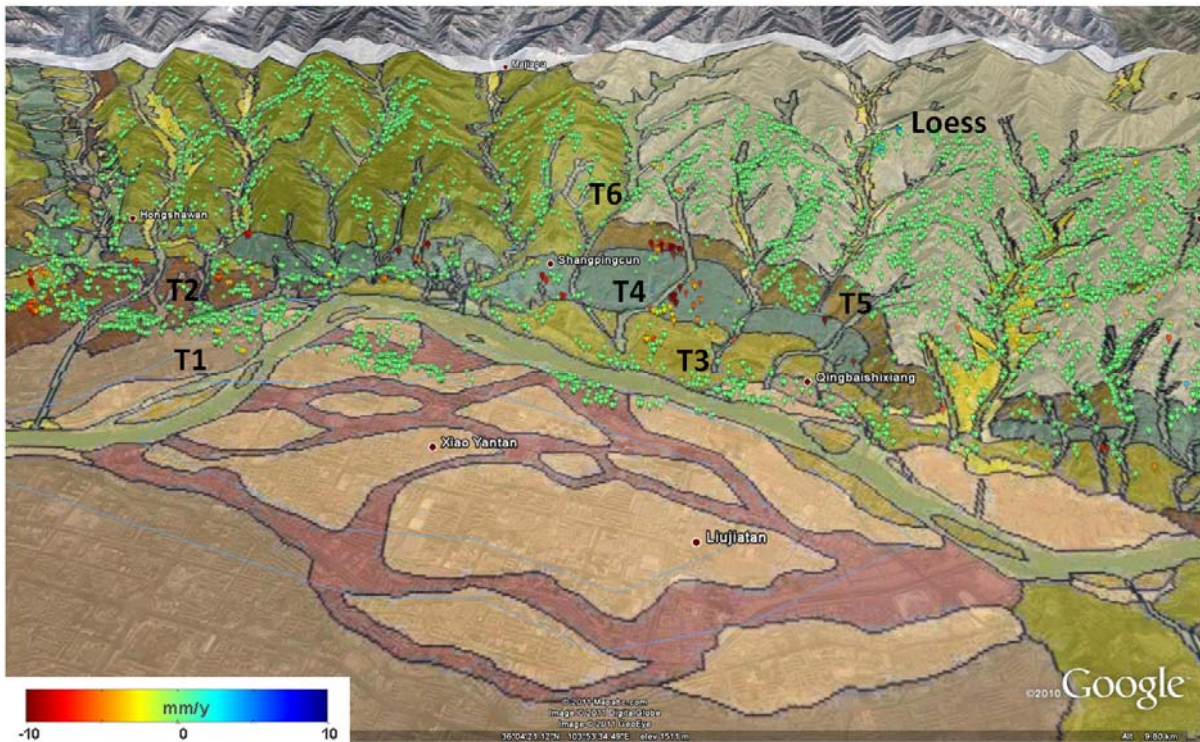


Figure 6. Google Earth-aided visualization of the PS velocities in the loess terrain and on the Yellow River terraces (eastern part of Lanzhou). Geomorphology is after [1]; see Legend in Fig. 2. Note general stability of the lower, flat areas with floodplain and valley-fill fluvial and alluvial deposits (Holocene terraces) and concentrations of moving PS on topographically higher and older (Late Pleistocene) terraces (particularly T3, T4 and T5).

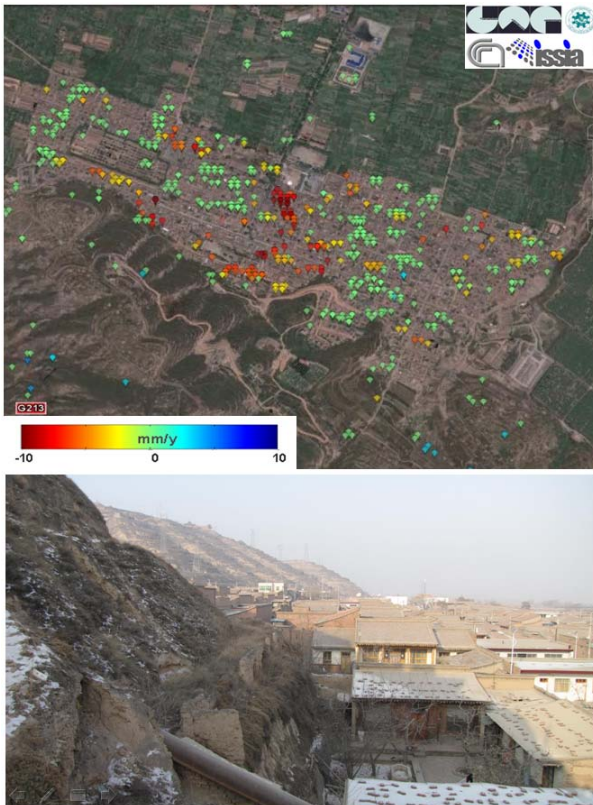


Figure 7. Example of detected movements in a small satellite town in the western periphery of Lanzhou. (upper) PS mean LOS velocity map superimposed on Google Earth optical image; velocity is saturated between -10 mm/y (red) and 10 mm/y (dark blue). (lower) Photo showing the town built on terrace T4 covered by collapsible Malan loess; note steep terrace riser to the left.

6. DISCUSSION AND CONCLUSIONS

The PSI processing of ENVISAT ASAR data produced spatially dense information (more than 400 PS/km²) on ground surface displacements in the Lanzhou territory. The PSI results interpreted in the geomorphological and geological context of the Yellow River valley indicate that the lower, flat areas with floodplain and valley-fill deposits (Holocene terraces with mainly reworked loess at the surface) are stable. This is good news, because the major part of the city of Lanzhou is built on these areas. On the other hand, some higher, gently sloping areas of the river valley appear locally unstable, particularly where the Late Pleistocene terraces are covered by aeolian loess.

Furthermore, PS with higher velocities appear to occur predominantly on topographically higher (and older) terraces (especially on the 4th and 5th order). Local clustering of moving PS along the steep terraces risers denotes their instability. Some PS movements are also

locally observed on steep slopes in collapsible, aeolian loess.

In addition, higher velocity PS also appear to be clustered around areas of poor drainage and/or irrigation (e.g. Dongpingcun in West Lanzhou). Indeed, it is well known that loess materials are subject to failure following increases in moisture content ([4], [5]). This observation is supported by, e.g. the landslide history of the 4th Yellow River terrace at Heifantai (some 20 km west of the current study area), where irrigation has caused large slope failures in the past and as recently as April 2011.

Importantly, the PSI results indicate that the 4th and 5th order (and to a lesser extent the 3rd order) Yellow River terraces have the highest relative susceptibility to ground failure. This is consistent with these terraces being covered by the late Pleistocene Malan loess, which is characterized by poor geotechnical properties ([1], [4]). The presence of highly plastic clays in the bedrock materials underlying the Lanzhou loess forms an additional factor influencing the spatial distributions of slope instability. There are also indications that the stability of these terraces depends on their recent development history and land use (especially when irrigation is involved).

Our reconnaissance field checks indicate that many of the detected movements could be associated with processes involving ground settlement/structure instability. However, loess materials are known to be characterized by relatively small pre-failure strains and typically brittle failures. Therefore, capturing of pre-failure strains loess terrain remains difficult.

Furthermore, it may often be difficult to ascertain the exact origin of low strain rates, especially when these are detected on slopes. Indeed, mm-cm/yr ground surface deformations detected by PSI can arise from different causes including subsidence and local settlements, shallow seasonal creep, pre-failure strains of incipient landslides, volumetric changes of geological/artificial materials, tectonics, and instability of structures that act as radar targets (e.g. [6]). Despite these interpretative difficulties, this case history shows once again that the PSI displacement results offer unique information, which, following expert judgment and correlations with information on local geology, geomorphology and slope history, can be used for wide-area and site-specific assessments of relative susceptibility to ground and slope instabilities.

ACKNOWLEDGEMENTS

ENVISAT images were provided by ESA in the framework of CAT-1 project #7444 "Exploitation of ENVISAT radar data for ground and infrastructure instability hazard assessments in the Lanzhou area (Gansu Province, China)", PI - J. Wasowski. We also

thank Jianjun, Xiao Li, Runqiang and Yating who helped in the field reconnaissance.

REFERENCES

- [1] Derbyshire, E., Meng, X.M. & Dijkstra, T.A. (Eds) 2000. *Landslides in the thick loess terrain of northwest China: mechanisms and mitigation*. John Wiley and Sons, Ltd, Chichester, pp 288.
- [2] Bovenga, F., Refice, A., Nutricato, R., Guerriero, L. & M.T. Chiaradia (2004), "SPINUA: a flexible processing chain for ERS/ENVISAT long term interferometry," in *Proceedings of Envisat & ERS Symposium, ESA SP- 572, CD-ROM, Salzburg, Austria*. 6-10 September 2004.
- [3] Bovenga, F., Nutricato, R., Refice A., & Wasowski, J. (2006). Application of Multi-temporal Differential Interferometry to Slope Instability Detection in Urban/Peri-urban Areas. *Engineering Geology, Special Issue on Remote sensing and ground-based geophysical techniques for recognition, characterisation and monitoring of unstable slopes*, 88(3-4), 218-239.
- [4] Dijkstra, T.A., Smalley, I.J. & C.D.F. Rogers (1995). Particle packing in loess deposits and the problem of structural collapse and hydroconsolidation, *Engineering Geology*, 40, 49-64.
- [5] Rogers, C.D.F., Dijkstra, T.A., & Smalley, I.J. (1994). Hydroconsolidation and subsidence of loess: studies from China, Russia, North America and Europe. *Engineering Geology*, 37, 83-113.
- [6] Colesanti, C., & Wasowski, J. (2006). Investigating landslides with space-borne Synthetic Aperture Radar (SAR interferometry). *Engineering Geology, Special Issue on Remote sensing and ground-based geophysical techniques for recognition, characterisation and monitoring of unstable slopes*, 88(3-4), 173-199.